LETTER

ACS chemical biology

Enzymatic Tailoring of Enterobactin Alters Membrane Partitioning and Iron Acquisition

Minkui Luo[†], Hening Lin[‡], Michael A. Fischbach[‡,§], David R. Liu[§], Christopher T. Walsh[‡,*], and John T. Groves[†,*]

[†]Department of Chemistry, Princeton University, Princeton, New Jersey 08544, [‡]Department of Biological Chemistry and Molecular Pharmacology, Harvard Medical School, Boston, Massachusetts 02115, and [§]Department of Chemistry & Chemical Biology, Harvard University, Cambridge, Massachusetts 02138

ABSTRACT Enterobactin (Ent), a prototypic bacterial siderophore, is modified by both the *C*-glucosyltransferase IroB and the macrolactone hydrolase IroE in pathogenic bacteria that contain the *iroA* cluster. To investigate the possible effects of glucosylation and macrolactone hydrolysis on the physical properties of Ent, the membrane affinities and iron acquisition rates of Ent and Ent-derived siderophores were measured. The data obtained indicate that Ent has a high membrane affinity ($K_x = 1.5 \times 10^4$) similar to that of ferric acinetoferrin, an amphiphile containing two eight-carbon hydrophobic chains. Glucosylation and macrolactone hydrolysis decrease the membrane affinity of Ent by 5–25-fold. Furthermore, in the presence of phospholipid vesicles, the iron acquisition rate is significantly increased by glucosylation and macrolactone hydrolysis, due to the resultant decrease in membrane sequestration of the siderophore. These results suggest that IroB and IroE enhance the ability of Ent-producing pathogens to acquire iron in membrane-rich microenvironments.

Iron is essential for growth in nearly all bacteria. In microenvironments where iron (largely present as Fe^{3+} in aerobic settings) is limiting, bacteria respond by activating genes required for synthesis and export of iron chelators known as siderophores, as well as membrane receptors and other proteins for the subsequent import of iron–siderophore complexes (*1, 2*). Many siderophores are small, nonribosomal peptide scaffolds containing catechols, hydroxamates, α-hydroxy acids, and similar bidentate functional groups to chelate ferric iron (*1, 2*).

A prime example of a catechol-containing siderophore is enterobactin (Ent; Figure 1), produced by Gram-negative enteric bacteria such as *Escherichia coli* and *Salmonella typhimurium*. With a K_d of 10^{-49} M for the hexadentate coordination of Fe^{3+} (*3*), Ent, the cyclic trilactone of *N*-2,3-dihyroxybenzoyl-L-serine, appears admirably engineered for removing ferric iron from vertebrate proteins such as transferrin during infection. However, the mammalian proteins serum albumin (*4*) and siderocalin (*5*) bind apo- and ferric (Fe)-Ent, respectively, thereby suppressing bacterial growth in various mammalian microenvironments. Siderocalin can also bind several other siderophores in the same site (*6*).

Various pathogenic strains of *E. coli* and *Salmonella* that harbor the *iroA* gene cluster can overcome the antimicrobial effects of serum proteins by enzymatic tailoring of Ent (*7, 8*). Modification of the Ent scaffold is effected by the *C*-glucosyltransferase IroB, which transfers a glucosyl moiety from UDP-glucose to C5 of each of the 2,3-dihydroxybenzoyl rings of Ent. This yields monoglucosyl enterobactin (MGE) and the corresponding diglucosyl (DGE) and triglucosyl (TGE) forms of the siderophore (Figure 1) (*9*). DGE, but not MGE or TGE, has been detected in the culture broth of *iroA*-harboring *Salmonella* (*7, 8*).

There are at least three consequences of siderophore *C*-glucosylation. First, the unusual *C*-glycosidic linkage is stable to hydrolysis in contrast to an *O*-glycosidic linkage. Second, the hydrophobicity of the scaffold is decreased by the hydrophilic glucosyl moieties in MGE and DGE. Third, and perhaps most importantly, glucosylation is likely to block binding and sequestration of Fe-MGE and Fe-DGE by siderocalin (*5, 10*), leaving these siderophores available for import by bacterial cells. We have suggested that the IroB-mediated tailoring of the periphery of enterobactin may be a bacterial counterattack against the host's innate immune system (*9*).

The five-gene *iroA* cluster also consists of *iroC*, *iroN*, *iroD*, and *iroE*. IroC and IroN are thought to be involved in export of apo-MGE/DGE and/or uptake of Fe-MGE/DGE. We have demonstrated that IroD is a cytoplasmic esterase that hydrolyzes both apo- and Fe-MGE/DGE to fragments with lower affinity for Fe^{3+} (*11*). Likewise, we have shown that IroE is a hydrolase, but unlike IroD, IroE is periplasmic and cleaves apo-MGE/DGE only once to produce linearized versions of these

*To whom correspondence should be addressed.
E-mail: christopher_walsh@hms.harvard.edu; jtgroves@princeton.edu.

Received for review September 28, 2005 and accepted January 3, 2006

Published online January 27, 2006

10.1021/cb0500034 CCC: $33.50

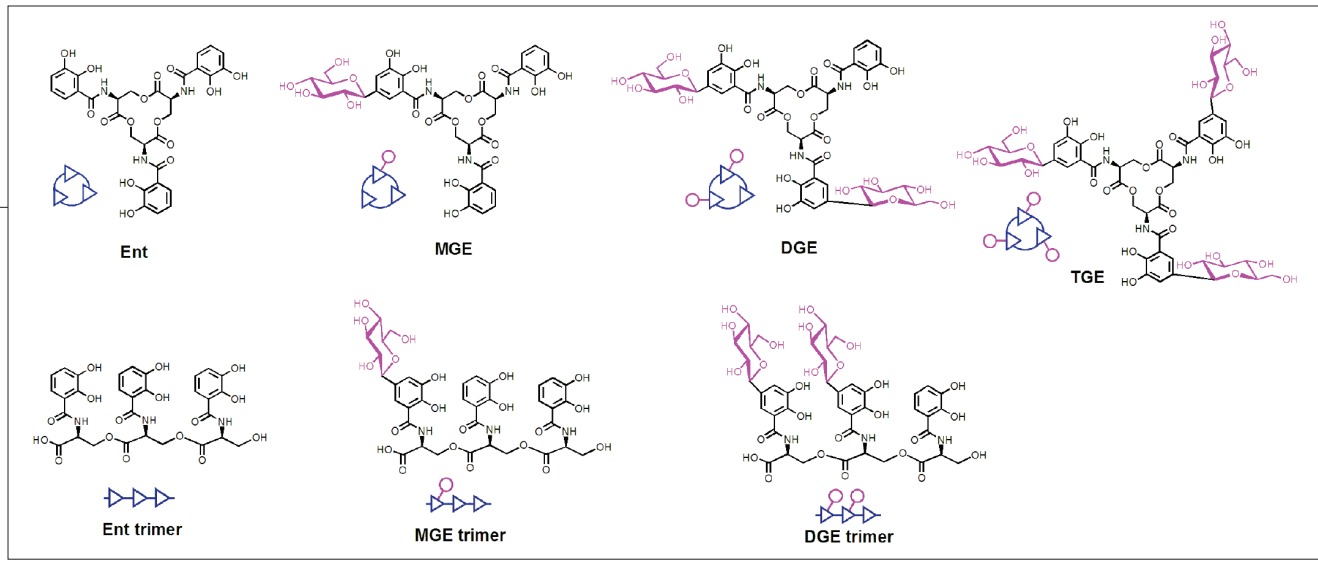

Figure 1. Chemical structures of Ent family siderophores used in this study. IroB-catalyzed glycosylation of Ent produces mono-, di-, and tri-glucosylated Ent (MGE, DGE, and TGE, respectively). In turn, IroD-catalyzed hydrolysis of Ent, MGE, and DGE produces their linear trimers.

siderophores (Figure 2; *11*). Indeed, a suite of siderophore species is found in the culture broth of *iroA*-harboring *Salmonella*; these include macrocyclic and linearized Ent and DGE and smaller hydrolytic fragments of each (*8, 12*). The linear trimer of Ent also has high affinity for ferric iron ($\Delta G = -8.9$ kcal mol^{-1}), although with a higher entropic barrier for hexadentate coordination (*13, 14*). The biological significance of IroE's enzymatic action (namely, why the bacteria would want to linearize the siderphores prior to their release) is thus very interesting. We hyphothesized that IroB/IroE-catalyzed tailoring of Ent by producing pathogens could affect Fe^{3+} binding kinetics and the hydrophobicity of this siderophore. In this study, we used

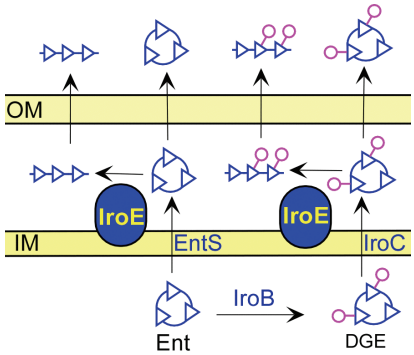

Figure 2. The tandem action of IroB and IroE creates a suite of siderophores that are secreted into the culture medium. IroB glycosylates Ent in the cytoplasm, forming DGE. Ent is transported to the periplasm by EntS, while IroC is proposed to transport DGE to the same compartment. IroE then hydrolyzes these trilactones, generating their linearized derivatives.

a membrane partitioning assay we have recently developed to investigate both possibilities (*15, 16*).

The membrane partition coefficients (K_x) of the apo-siderophores were determined from observed changes in the rates of iron acquisition (k_{obs}) as the phospholipid membrane concentration of the medium was varied. The k_{obs} values for all siderophore species tested are similar (0.033–0.058 mM^{-1} s^{-1}) (Table 1). The rates of iron acquisition by Ent and its derivatives were determined to be due to a direct interaction of the siderophores with iron citrate. An alternative mechanism involving rate-limiting dissociation of iron from the iron citrate cluster can be ruled out on several grounds. The series of experiments were carried out with a 20-fold excess of iron. Although rate-limiting iron release from iron citrate has been reported, such a process was observed only in the presence of high siderophore to iron ratios (*17*). The iron-chelation kinetics of Ent and its derivatives reported here show excellent pseudo-first-order fits of concentration of chelator versus time with a half-time around 20 s (Supplementary Figure 1). By contrast, an iron-dissociation-controlled process would be zero-order in concentration of Ent and would show a linear relationship with a half-life of several hours (*18*). Consequently, we conclude that glycosylation, linearization, and the attendant introduction of a carboxylate functionality do not hinder the facility of Fe^{3+} ligation by Ent.

In contrast, the membrane partition coefficients (K_x) showed substantial variation among the siderophore species. Ent shows a remarkable affinity for membranes with a K_x value of 15000, similar to the value we have found for Fe-acinetoferrin, a siderophore amphiphile with two eight-carbon side chains (*16*). The addition of one (MGE) or two (DGE) *C*-glucosyl units decreased K_x only by ~5-fold, and addition of three (TGE) *C*-glucosyl units decreased K_x to about 1/10 that of Ent, consistent with the hydrophilic nature of the sugars. Correspondingly, monohydrolysis of the Ent trilactone to a linear trimer with one carboxylate decreased its K_x 25-fold, and hydrolysis of DGE decreased its K_x more than 10-fold. It has been observed that Ent, after being synthesized, is not secreted efficiently because it accumulates in the periplasm (*19*), The high K_x value of Ent, which was unrecognized prior to this report, could partially explain this observation and suggests that glucosylation by IroB and macrolactone linearization by IroE could be strategies to increase secretion efficiency.

We further show that Ent binds ferric iron significantly more slowly in the presence of lipid membranes than it does in membrane-free aqueous solution, due to the high partition ratio into the membrane phase and out of the aqueous medium (Table 1 and Figure 3). This decrease in iron acquisition rate is a consequence of the lower mole fraction of Ent in aqueous solution and, thereby, inefficient access to the iron source. This result is consistent with

TABLE 1. Ferric iron acquisition rate constants and membrane partitioning coefficients

	Ent	Ent trimer	MGE	MGE trimer[a]	DGE	DGE trimer[a]	TGE
Iron acquisition rate constant (k_{obs}, mM^{-1} s^{-1})[b]	0.041	0.058	0.042	0.048	0.045	0.048	0.033
Membrane partitioning coefficient (K_x)	15000	490	3400	640	3100	230	1400
Relative iron acquisition rate with 10 mM lipid[c]	0.27	0.92	0.62	0.90	0.64	0.96	0.81

[a]The MGE and DGE linear trimers were obtained by IroD-catalyzed regioselective hydrolysis of MGE and DGE and are different from the linear trimers that can be obtained with IroE, which is not regioselective. However, we obtained similar results using the mixture of linear trimers generated by IroE-catalyzed MGE or DGE hydrolysis. [b]This is the iron acquisition rate measured in the absence of phospholipids vesicles. [c]These data were obtained by dividing the iron acquisition rate in the presence of lipid by that in the absence of lipid. The iron acquisition rates in the absence of lipid are defined as 1.

the reported observation that *E. coli* strains producing Ent but not aerobactin scavenge transferrin-bound (extracellular) iron more efficiently than cellular iron (*20*). Hydrolytic linearization and glucosylation suppress partitioning of Ent into the membrane phase and result in higher rates of iron acquisition. Therefore, it may be advantageous for siderophore-producing bacteria to secrete a suite of iron chelators that cover a range of membrane affinities and hydrophobicities.

The tandem action of IroB and IroE creates just such a suite of siderophores. These glucosylated and linearized Ent derivatives partition more efficiently into the aqueous phase and thus may forage more effectively for ferric iron in a mammalian host. For the marinobactin (*15, 21*), aquachelin (*21*), and amphibactin (*22*) siderophores, a convergent tailoring strategy is employed. These hydrophilic tetra- to hexapeptide scaffolds are enzymatically acylated at their amino termini, thus converting them to lipophilic amphiphiles through the introduction of fatty acyl substituents to the iron-binding peptide core (*23*). The acyltransferases responsible for these modifications evidently show promiscuity for the acyl-ACP substrate, again to create a suite of siderophores with a range of hydrophobicities. Similarly, mycobacteria produce siderophores with a range of hydrophobicities (*24*). The most hydrophobic of these, mycobactin, has been shown recently to permeate cell membranes to extract iron from target cells such as macrophages (*25*). It is also clear that profound changes in the conformation of siderophores such as acinetoferrin (*26*) and rhizobactin (*27*) upon binding iron transform the properties of these molecules such that while the apo-forms are tuned for iron prospecting, the iron-bound forms become homing devices for the bacterial membrane receptor. Taken together with the *iroA* system, bacteria have elaborated a series of enzymatic tailoring strategies to control the hydrophobic/hydrophilic balance of siderophores. The capacity to add either hydrophilic (glucosyl) or hydrophobic (fatty acyl) groups to nonribosomal peptide scaffolds represents two convergent strategies to titrate the physical properties of a set of siderophores that scavenge the essential ferric iron nutrient.

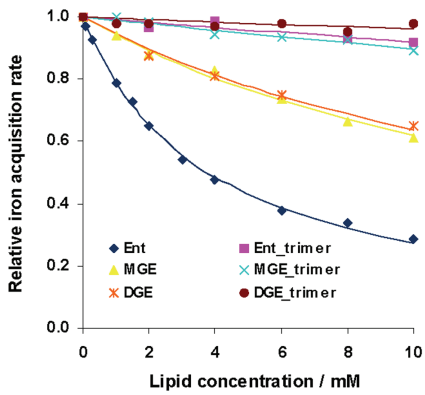

Figure 3. The iron-acquisition kinetics and membrane partitioning of Ent-derived siderophores. Relative Fe^{3+} binding rates of Ent-derived siderophores (50 μM) from 1 mM ferric ammonium citrate at 37 °C and pH 7.5 were determined in the presence of varied lipid vesicle concentration by monitoring the appearance of the ferric catecholate chromophore at 490 nm.

METHODS

Preparation of Siderophores. Ent, MGE, DGE, TGE, and the linearized trimers from IroD-catalyzed MGE/DGE hydrolysis were prepared as described previously (*11*). IroD was used because it catalyzes the hydrolysis of MGE/DGE regioselectively and gives only one linear trimer isomer as the major hydrolysis product. Ent linear trimer was prepared using IroE N-30 catalyzed hydrolysis because there is no regioselectivity issue and IroE affords almost exclusively the linear trimer product. Since IroD and IroE give different regioisomers of linear trimer products for MGE/DGE hydrolysis, we also prepared MGE/DGE linear trimers using IroE-catalyzed hydrolysis to make sure that different regioisomers have similar membrane affinities and iron acquisition rates. The hydrolysis of Ent/MGE/DGE with IroE was carried out with 128 mM Ent/MGE/DGE, 40 nM IroE N-30, in 50 mL of 75 mM HEPES buffer pH 7.5 for 1 h. The reaction mixture was quenched with 25 mL of 2.5 N HCl in methanol (prepared by mixing 10 mL of concentrated HCl with 40 mL of methanol), and the hydrolysis products were purified by reverse phase HPLC using a gradient of 0–40% acetonitrile, with the aqueous phase containing 0.1% (v/v) trifluoroacetic acid. The HPLC fractions were lyophilized, and the linear trimer products were dissolved in DMSO. The concentrations of the resulting solutions were determined using HPLC by co-injecting equal volumes of the solutions with a known concentration Ent solution and comparing the areas of absorption at 316 nm.

Preparation of Lipid Vesicles. Unilamellar vesicles were prepared as previously described (*15, 16*) by sonication for small unilamellar vesicles (SUV) with a diameter of 30–40 nm. Briefly, weighed 1,2-dimyristoyl-*sn*-glycero-3-phosphocholine (DMPC, from Avanti Polar

Lipids) was dissolved in chloroform and then transferred into 5-mL test tubes. The thin films of lipid were deposited on the walls of the test tubes after evaporating the solvent with a stream of argon and then were subjected to high vacuum overnight. The dried lipid films were hydrated in HEPES buffer (100 mM HEPES, 150 mM NaCl) at 40 °C for 30 min. The pretreated lipid buffers were sonicated with a probe tip sonicator in an ice–water bath until the ice was melted completely and the bath temperature had reached room temperature (taking about 30 min). After centrifugation of the vesicle suspension at 12,000 rpm for 5 min to remove the sonicator tip debris, a translucent SUV suspension was obtained.

Measurement of Iron-Acquisition Rates and Membrane Affinities. A Hi-Tech SF-61 DX2 stopped-flow spectrophotometer with the photomultiplier absorbance mode was used for kinetic measurements of siderophore-mediated iron acquisition from ferric ammonium citrate (FAC, from Aldrich-Sigma Inc.) at 37 °C. Briefly, one mixing syringe was filled with FAC stock solution and the other one was loaded with the siderophore solution containing various concentrations of lipid vesicles (1 mM FAC, 50 μM siderophore, and 0–10 mM DMPC SUV for final concentrations). Upon mixing, the changes of the absorbance at 490 nm were measured versus time. The pseudo-first-order rate constants were obtained upon fitting a general exponential equation (eq 2) using Scientist software. The second-order rate constants (k_{obs} in Table 1) were derived by dividing the pseudo-first-order rate constants by the concentration of FAC (1 mM).

The partition coefficients (K_x) of all compounds tested were obtained on the basis of the kinetic relationship (eq 1.1) between the relative rates for siderophore-mediated iron acquisition from FAC (k_{obs}/k_w) and the DMPC SUV concentration ([Vesicle]). Here α is the ratio (k_v/k_w) of the lipid-phase iron-mobilization rate (k_v) to the aqueous-phase rate (k_w); k_w and k_{obs} correspond to the rates of siderophore-mediated iron acquisition from FAC in the absence or presence of the various concentrations of DMPC SUV, respectively. k_w and k_{obs} were derived from eq 2, where A_t is the absorbance changes at 490 nm versus time t, A_{obs} is the maximal absorption change, and C is the initial absorption. Equation 1.1 is derived from eq 1.2, which we have reported previously (*16*). The difference between eqs 1.1 and1.2 lies in the value of α, which is set as zero for the former and a variable parameter for the latter. For Ent, the two equations give results almost identical with $K_x = 1.5 \times 10^4$ for eq 1.1 (Figure 3), and $K_x = 1.6 \times 104$ and near-zero α ($\alpha = 0.03$, data not shown) for eq 1.2. For DGE, MGE, DGE trimer, and MGE trimer, only eq 1.1 can produce a reasonable fit because of the relatively low membrane affinities of these siderophores. Consequently, all partition coefficients were obtained on the basis of eq 1.1, in which $\alpha = 0$ was arbitrarily used. This lipid-concentration-dependent hyperbolic relationship arises from siderophore-mediated membrane partitioning, since the rate of iron mobilization from FAC is close to zero in the lipid phase in contrast to non-zero k_w in the aqueous phase.

$$\frac{k_{obs}}{k_w} = \frac{[\text{Water}]}{K_x \times [\text{Vesicle}] + [\text{Water}]} \quad (1.1)$$

$$\frac{k_{obs}}{k_w} = (\alpha - 1)\frac{K_x \times [\text{Vesicle}]}{K_x \times [\text{Vesicle}] + [\text{Water}]} \quad (1.2)$$

$$A_1 = A_{obs}[1 - \exp(-k_{obs} \times t)] + C \quad (2)$$

Acknowledgment: This work was supported in part by the National Science Foundation through the Environmental Molecular Science Institute, CEBIC at Princeton University, CHE-0221978 (J.T.G.) and CHE-0316301 (J.T.G.), NIH AI 47238 (C.T.W.), NIH R01GM065400 (D.RL.), a postdoctoral fellowship from the Jane Coffin Childs Memorial Fund (H.L.), and a graduate fellowship from the Hertz Foundation (M.A.F.).

Supporting Information Available: This material is available free of charge via the Internet.

REFERENCES

1. Neilands, J. B. (1995) Siderophores: Structure and function of microbial iron transport compounds, *J. Biol. Chem. 270*, 26723–26726.
2. Crosa, J. H., and Walsh, C. T. (2002) Genetics and assembly line enzymology of siderophore biosynthesis in bacteria, *Microbiol. Mol. Biol. Rev. 66*, 223–249.
3. Loomis, L. D., and Raymond, K. N. (1991) Solution equilibria of enterobactin and metal-enterobactin complexes, *Inorg. Chem. 30*, 906–911.
4. Konopka, K., and Neilands, J. B. (1984) Effect of serum albumin on siderophore-mediated utilization of transferrin iron, *Biochemistry 23*, 2122–2127.
5. Goetz, D. H., Holmes, M. A., Borregaard, N., Bluhm, M. E., Raymond, K. N., and Strong, R. K. (2002) The neutrophil lipocalin NGAL is a bacteriostatic agent that interferes with siderophore-mediated iron acquisition, *Mol. Cell. 10*, 1033–1043.
6. Holmes, M. A., Paulsene, W., Jide, X., Ratledge, C., and Strong, R. K. (2005) Siderocalin (Lcn 2) also binds carboxymycobactins, potentially defending against mycobacterial infections through iron sequestration, *Structure 13*, 29–41.
7. Hantke, K., Nicholson, G., Rabsch, W., and Winkelmann, G. (2003) Salmochelins, siderophores of *Salmonella enterica* and uropathogenic *Escherichia coli* strains, are recognized by the outer membrane receptor IroN, *Proc. Natl. Acad. Sci. U.S.A. 100*, 3677–3682.
8. Bister, B., Bischoff, D., Nicholson, G. J., Valdebenito, M., Schneider, K., Winkelmann, G., Hantke, K., and Sussmuth, R. D. (2004) The structure of salmochelins: C-glucosylated enterobactins of *Salmonella enterica*, *Biometals 17*, 471–481.
9. Fischbach, M. A., Lin, H., Liu, D. R., and Walsh, C. T. (2005) In vitro characterization of IroB, a pathogen-associated C-glycosyltransferase, *Proc. Natl. Acad. Sci. U.S.A. 102*, 571–576.
10. Flo, T. H., Smith, K. D., Sato, S., Rodriguez, D. J., Holmes, M. A., Strong, R. K., Akira, S., and Aderem, A. (2004) Lipocalin 2 mediates an innate immune response to bacterial infection by sequestrating iron, *Nature 432*, 917–921.
11. Lin, H., Fischbach, M. A., Liu, D. R., and Walsh, C. T. (2005) In vitro characterization of salmochelin and enterobactin trilactone hydrolases IroD, IroE, and Fes, *J. Am. Chem. Soc. 127*, 11075–11084.
12. Zhu, M., Valdebenito, M., Winkelmann, G., and Hantke, K. (2005) Functions of the siderophore esterases IroD and IroE in iron-salmochelin utilization, *Microbiology 151*, 2363–2372.
13. Scarrow, R. C., Ecker, D. J., Ng, C., Liu, S., and Raymond, K. N. (1991) Iron(III) coordination chemistry of linear dihydroxyserine compounds derived from enterobactin, *Inorg. Chem. 30*, 900–906.
14. O'Brien, I. G., Cox, G. B., and Gibson, F. (1971) Enterobactin hydrolysis and iron metabolism in *Escherichia coli*, *Biochim. Biophys. Acta 237*, 537–549.
15. Xu, G., Martinez, J. S., Groves, J. T., and Butler, A. (2002) Membrane affinity of the amphiphilic marinobactin siderophores, *J. Am. Chem. Soc. 124*, 13408–13415.
16. Luo, M., Fadeev, E. A., and Groves, J. T. (2005) Membrane dynamics of the amphiphilic siderophore acinetoferrin, *J. Am. Chem. Soc. 127*, 1726–1736.
17. Faller, B., and Nick, H. (1994) Kinetics and mechanism of iron(III) removal from citrate by desferrioxamine B and 3-hydroxy-1,2-dimethyl-4-pyridone, *J. Am. Chem. Soc. 116*, 3860–3865.
18. Bates, G. W., Billups, C., and Saltman, P. (1967) The kinetics and mechanism of iron(III) exchange between chelates and transferrin, *J. Biol. Chem. 242*, 2810–2815.
19. Vartanian, M. D. (1988) Differences in excretion and efficiency of the aerobactin and enterochelin siderophores in a bovine pathogenic strain of *Escherichia coli*, *Infect. Immun. 56*, 413–418.
20. Brock, J. H., Williams, P. H., Liceaga, J., and Wooldridge, K. G. (1991) Relative availability of transferrin-bound iron and cell-derived iron to aerobactin-producing and enterochelin-producing strains of *Escherichia coli* and to other microorganisms, *Infect. Immun. 59*, 3185–3190.
21. Martinez, J. S., Zhang, G. P., Holt, P. D., Jung, H.-T., Carrano, C. J., Haygood, M. G., and Butler, A. (2000) Self-assembling amphiphilic siderophores from marine bacteria, *Science 287*, 1245–1247.
22. Martinez, J. S., Carter-Franklin, J. N., Mann, E. L., Martin, J. D., Haygood, M. G., and Butler, A. (2003) Bioinorganic Chemistry Special Feature: Structure and membrane affinity of a suite of amphiphilic siderophores produced by a marine bacterium, Proc. *Natl. Acad. Sci. U.S.A. 100*, 3754–3759.
23. Groves, J. T. (2003) Bioinorganic Chemistry Special Feature: The bioinorganic chemistry of iron in oxygenases and supramolecular assemblies, *Proc. Natl. Acad. Sci. U.S.A. 100*, 3569–3574.
24. Ratledge, C. (2004) Iron, mycobacteria and tuberculosis, *Tuberculosis 84*, 110–130.
25. Luo, M., Fadeev, E. A., and Groves, J. T. (2005) Mycobactin-mediated iron acquisition within macrophages, *Nat. Chem. Biol. 1*, 149–153.
26. Fadeev, E. A., Luo, M., and Groves, J. T. (2004) Synthesis, structure, and molecular dynamics of gallium complexes of schizokinen and the amphiphilic siderophore acinetoferrin, *J. Am. Chem. Soc. 126*, 12065–12075.
27. Fadeev, E. A., Luo, M., and Groves, J. T. (2005) Synthesis and structural modeling of the amphiphilic siderophore rhizobactin-1021 and its analogs, *Bioorg. Med. Chem. Lett. 15*, 3771–3774.